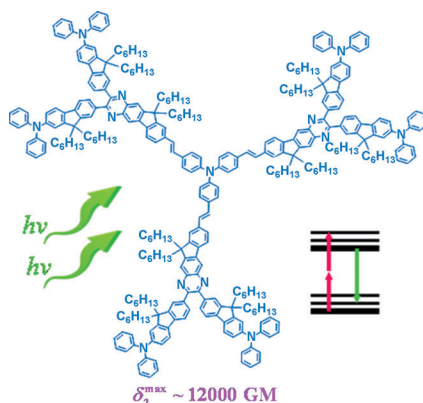


FULL PAPER

In pole position: Two multipolar chromophores that were derived from 2,3,8-functionalized indenoquininoxaline units manifest strong and wide dispersed two-photon absorption (2PA) in the NIR region under the irradiation of femtosecond laser pulses. Moreover, these model fluorophores could act as effective power-limiters/stabilizers against nanosecond laser pulses within the same spectroscopic regime.



Two-Photon Chromophore

Tzu-Chau Lin,* Fang-Ling Guo,
May-Hui Li, Che-Yu Liu — ■■■■—■■■■

Degenerate Two-Photon Absorption and Effective Optical-Power-Limiting Properties of Multipolar Chromophores Derived from 2,3,8-Trisubstituted Indenoquininoxaline



DOI: 10.1002/asia.201300223

Degenerate Two-Photon Absorption and Effective Optical-Power-Limiting Properties of Multipolar Chromophores Derived from 2,3,8-Trisubstituted Indenoquinoline

Tzu-Chau Lin,* Fang-Ling Guo, May-Hui Li, and Che-Yu Liu^[a]

Abstract: Two analogous multipolar chromophores (**1** and **2**) that contained 2,3,8-trisubstituted indenoquinoline moieties have been synthesized and characterized for their two-photon absorption properties, both in the femto-second and nanosecond time regimes. We demonstrated that their multi-branched framework structures, which incorporated appropriately functional-

ized indenoquinoline units, afforded large molecular nonlinear absorptivities within the studied spectroscopic range. Effective optical-power-limiting and stabilization behaviors in the nano-

Keywords: absorption • chromophores • Heck reaction • indenoquinolines • nonlinear optics

second regime of dye molecule (**2**) were also investigated and the results indicated that such a structural motif could be a useful approach to the molecular design of highly active two-photon systems for quick-response and related broadband optical-suppressing applications, in particular for confronting laser pulses of a long duration.

Introduction

Degenerate two-photon absorption (2PA) processes can be achieved within a linearly transparent—but nonlinearly absorbing—medium through the simultaneous absorption of two photons at wavelengths far from the cutoff wavelength of the medium's linear absorption band. Although the theory of such a nonlinear optical phenomenon was first predicted by Göppert-Mayer in 1931,^[1] the lack of appropriate light sources at that time held back scientists from experimentally studying the details of this nonlinear process until the advent of lasers in the 1960s.^[2] Over the past two decades, the availability of stable and high-peak-power lasers has triggered further momentum in the exploration of two-photon-related technologies. In conjunction with the intrinsic quadratic dependence of the incident light intensity in the 2PA process, many potential applications in the emerging field of photonics and biophotonics have been proposed and explored, including optical-power limiting/stabilization, frequency up-converted lasing, 3D data storage, 3D micro-fabrication, nondestructive bio-imaging, and two-photon-assisted photodynamic therapy.^[3] Nevertheless, the relatively small two-photon-absorption cross-sections of commercially available materials have limited their widespread utility.

Therefore, the development of new organic compounds that exhibit highly efficient 2PA within a specific spectroscopic region is consequently in great demand. Based on the enormous efforts that have been made in the investigation of a wide range of molecular systems, it has been realized that the combination of several structural parameters, such as intramolecular charge-transfer efficiency and/or the effective size of a π -conjugation domain within a molecule, are closely related to the molecular 2PA.^[4–11] In other words, the arrangement of structural units plays a hinge role in the molecular design toward highly active 2PA chromophores. Among the previously investigated π systems, multi-branched structures seem to be a promising approach because they exhibit cooperative effects and lead to enhanced molecular 2PA, whilst maintaining a broad spectroscopic window of transparency.^[5a–e, 6, 7c, 8a–b, d, 9c–d, f, 10, 11] Moreover, branched skeletons also provide the opportunity for material chemists to combine disparate structural parameters into one molecule so that the resulting compound could manifest multi-functional character as desired for various practical concerns.

As part of our ongoing search for useful structural parameters in molecular design for enhancing two-photon-absorption properties of conjugated systems, we are interested in exploring the influence that may be caused by the electronic properties of the incorporated heterocyclic structures and the arrangement of the employed π units on the molecular 2PA when constructing multi-branched π structures. Herein, we report the synthesis of a new set of two-photon-active model chromophores (**1** and **2**) that were derived from multi-functionalized indenoquinoline moieties, as well as an initial investigation of their 2PA-related properties by

[a] Prof. T.-C. Lin, F.-L. Guo, M.-H. Li, C.-Y. Liu
Photonic Materials Research Laboratory
Department of Chemistry
National Central University
300 Jhong-da Rd. 32001 Jhong-Li (Taiwan)
Fax: (+886)3-4227664
E-mail: tclin@ncu.edu.tw

Supporting information for this article is available on the WWW under <http://dx.doi.org/10.1002/asia.201300223>.

using both femtosecond and nanosecond IR laser pulses as probing tools.

Results and Discussion

1. Molecular Structures and Syntheses

The chemical structures of the studied model compounds are shown in Figure 1. Compound **1** was constructed by attaching two diphenylaminofluorene units onto the C2 and C3 positions and one vinyltriphenylamine unit onto the C8 position of an indenoquinoxaline scaffold. The skeleton of compound **2** constitutes an expanded version of compound **1** because it possesses two additional functionalized indenoquinoxaline arms to form a symmetrically substituted dendritic π framework. Although the electron-deficient quinoxaline ring complex has been utilized as an acceptor to produce highly efficient bipolar luminescent materials,^[12] so far, there have only been a few reports on 2PA and/or χ^3

materials that contain quinoxalinyli moieties.^[13] Therefore, the use of quinoxaline or quinoxalinoind units in the design and synthesis of two-photon-active materials may be worthy of further exploration. Our original molecular-design strategies of these model chromophores were based on the idea of tentatively placing an elongated version of quinoxaline, that is, an indenoquinoxaline scaffold, between various electron-donating moieties with uneven electron-pushing strengths, so that the polarizability of the resulting fluorophores could be altered and tuned, owing to the manner of structural arrangement, and, hence, the whole molecule may possess larger multipolar character. Moreover, we attached alkyl chains onto the C9 positions of all of the fluorenyl units to enhance their molecular solubility in common organic solvents, which is another important issue to be considered in the molecular design, both in terms of experimentation and application.

The syntheses of the target model compounds, which mainly involve the preparation of the primary intermediates

(**6** and **11**) for the construction of an indenoquinoxaline ring complex (**13**), followed by one or three Pd-catalyzed Heck coupling reactions to furnish the target chromophores (**1** and **2**), are shown in Scheme 1. For the preparation of compound **6**, we employed a recently developed one-step Sonogashira reaction procedure^[14] to afford its diarylacetylene precursor first and then utilized KMnO_4 as the main oxidant for the preparation of the targeted diketone (**6**). For the synthesis of diamine **11**, a series of functional-group transformations starting from compound **3** was performed, as outlined in Scheme 1. The detailed syntheses, including the preparation of the major intermediates and the final catalytic coupling reactions toward the targeted model fluorophores, are described in the Experimental Section.

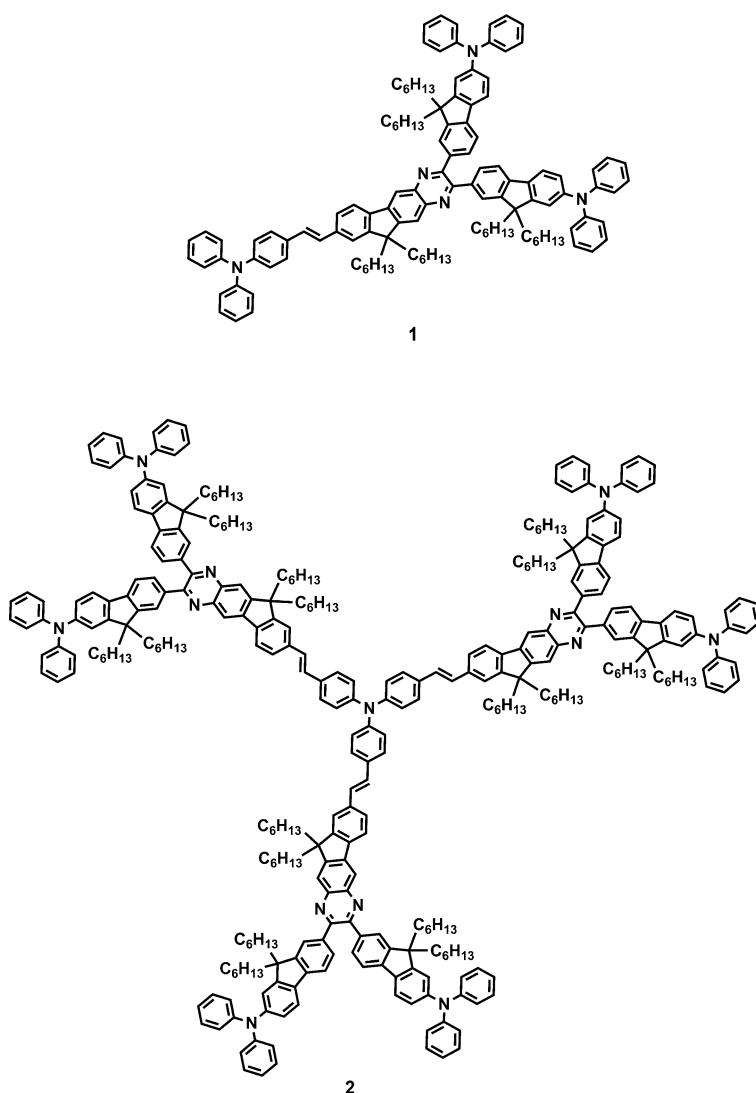
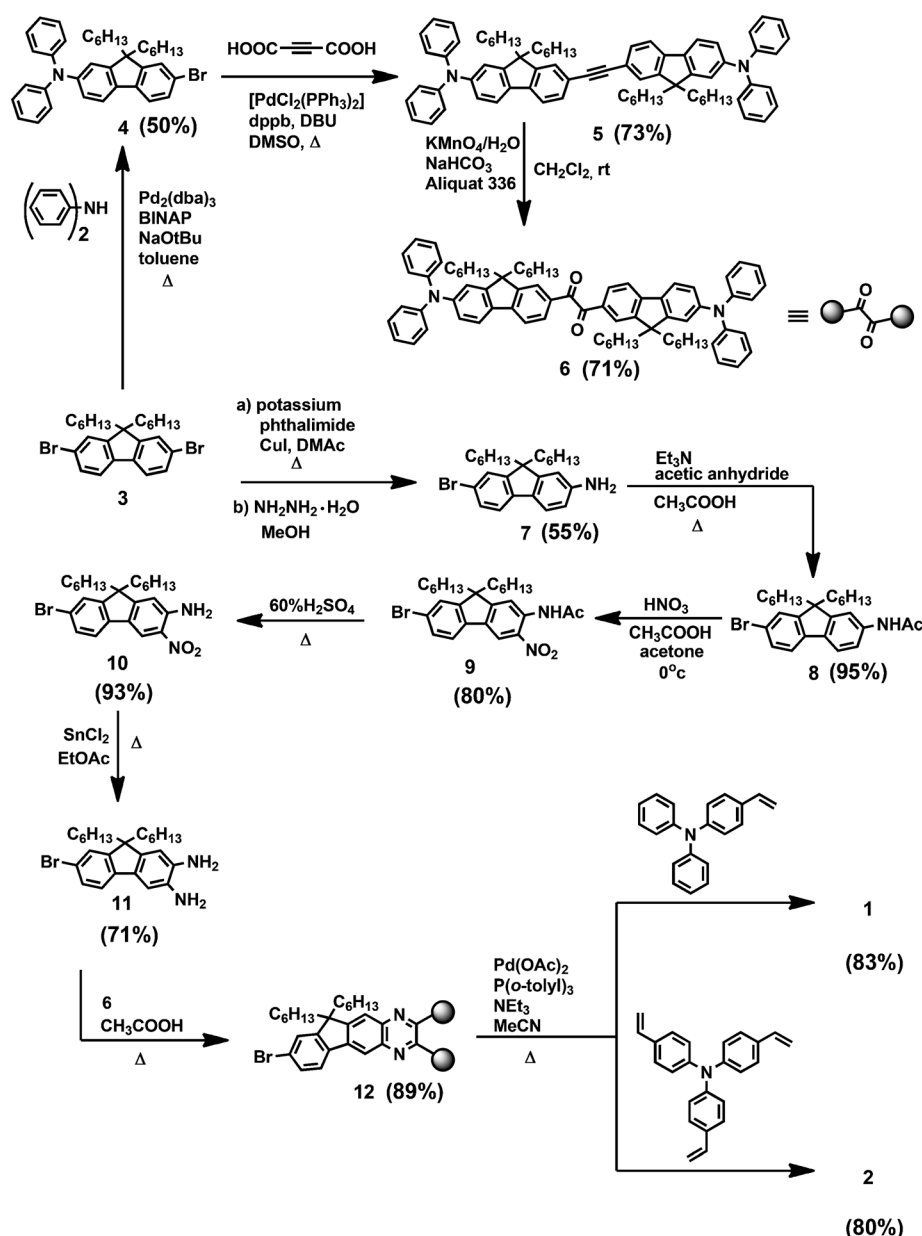


Figure 1. Molecular structures of the model chromophores.



Scheme 1. Synthesis of the key intermediates and final compounds (the yield for each compound is given in parentheses). BINAP = 2,2'-bis(diphenylphosphino)-1,1'-binaphthyl, dba = dibenzylideneacetone, DMAc = dimethylacetamide.

Figure 2. The 1PA spectra were recorded on a Shimadzu 3501 PC spectrophotometer and the 1PA-induced fluorescence spectra were recorded on a Jobin-Yvon FluoroMax-4 spectrometer. All of these chromophores exhibited strong linear absorption in the UV/Vis region with the lowest-energy peaks located at about 450 nm. The molar absorption coefficient (ϵ) is about $6.9 \times 10^4 \text{ cm}^{-1} \text{ M}^{-1}$ for compound **1** and about $2.42 \times 10^5 \text{ cm}^{-1} \text{ M}^{-1}$ for compound **2**. These dye solutions also emit intense green/yellowish fluorescence under the irradiation of a common UV lamp, in agreement with the measured emission spectra (Figure 2, inset). Chromophore **2** also exhibits strong solvent-polarity dependence of their fluorescence properties, including band positions

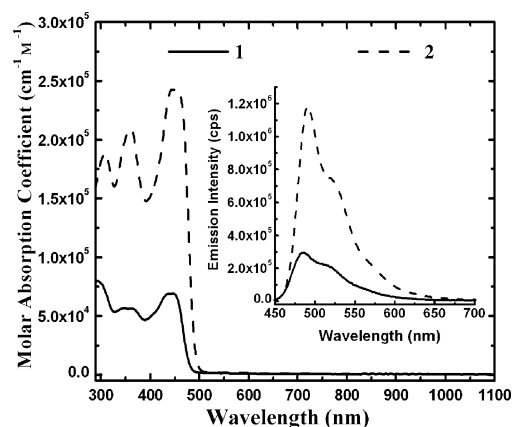


Figure 2. Linear absorption and fluorescence spectra (inset) of compounds **1** and **2** at a concentration of $1 \times 10^{-6} \text{ M}$ in toluene.

and lifetimes, as shown in Figure 3. Similar properties have been observed in other multi-branched symmetrical chromophore systems and, in those cases, the symmetry-breaking phenomenon as induced by electron-vibration coupling and dipolar solvation effects were proposed to account for this behavior.^[15]

The power-squared dependence of the 2PA-induced fluorescence intensity on the excitation intensity of these fluorophores was also investigated at a representative wavelength ($\lambda_{\text{ex}} \approx 800 \text{ nm}$). A wavelength-tunable mode-locked Ti:Sapphire laser (Chameleon Ultra II, Coherent), which delivered 140 fs pulses with a repetition rate of 80 MHz and a beam diameter of 2 mm, was utilized as an excitation light source for this experiment. Figure 4b,c shows the logarithmic plots of the experimental data and the results (slope of linear fit ≈ 2) confirm that the 2PA process is responsible for the observed up-converted fluorescence emissions in all cases. The temporal behavior and lifetimes of 1PA- and 2PA-induced fluorescence of the same sample solutions were also probed based on the time-correlated single-photon-counting (TCSPC) technique by

using a highly sensitive photomultiplier that was equipped with an accumulating real-time processor as the detection system (PMA-182 and TimeHarp 200, PicoQuant). The same Ti:sapphire laser system was employed for this experiment. The fluorescence-decay curves of solutions of the studied compounds are shown in the Supporting Information, Figure S3, over a 10 ns full scale for one- and two-photon excitation (in the femtosecond regime). Theoretical fitting of each decay curve to single-exponential dependence has revealed that, for each solution of the chromophore, identical 1PA/2PA-induced fluorescence lifetimes were observed, which indicated that this phenomenon was independent of the excitation

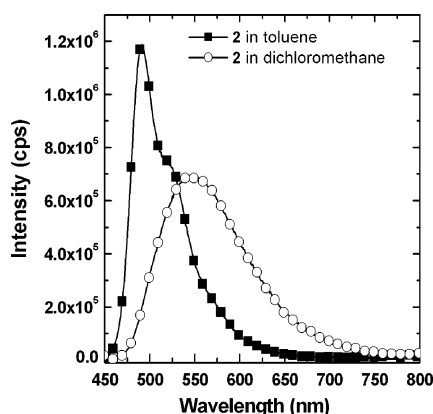


Figure 3. Fluorescence spectra of compound **2** in various solvents. For the color version of the spectra, with photographs that show the distinct color changes in compound **2** in different solvents, can be found in the Supporting Information. τ_{1PA-FL} : fluorescence lifetime, $\tau_{1PA-FL}=1.11$ and 2.18 ns in toluene and THF, respectively; concentration of compound **2** = 1×10^{-6} M in all cases.

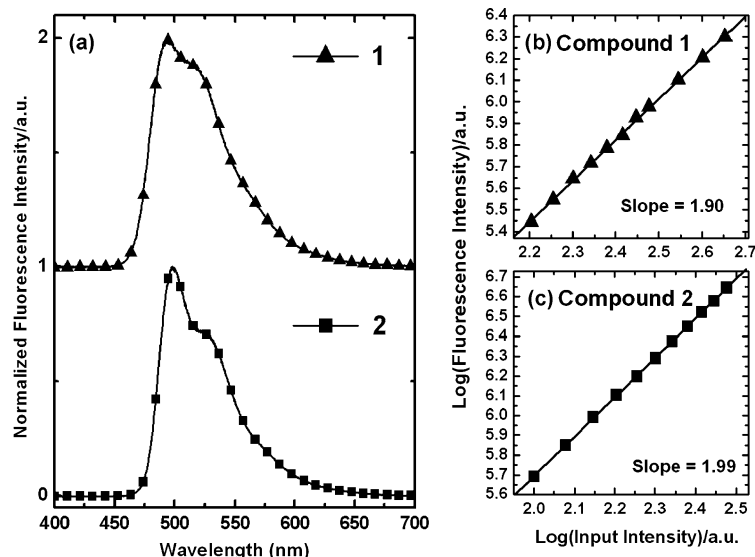


Figure 4. a) Normalized two-photon-excited upconversion spectra of fluorophores **1** and **2** at a concentration of 1×10^{-4} M in toluene. b, c) Logarithmic plots of the power-squared dependence of the 2PA-induced fluorescence intensity on the input intensity of these compounds in toluene.

Table 1. Photophysical properties of model chromophores **1** and **2** in toluene.^[a]

	$\lambda_{\max}^{\text{abs}}$ [nm] ^[b]	$\log \epsilon$ ^[c]	$\lambda_{\max}^{\text{em}}$ [nm] ^[d]	Φ_F ^[e]	δ_2^{max} [ns] ^[f]	τ_{2PA-FL} [ns] ^[g]	δ_2^{max} [GM] ^[h]	N_{eff}^{π} ^[i]	$\delta_2^{\text{max}}/N_{\text{eff}}^{\pi}$
1	446	4.84	486	0.70	1.3	1.3	3630	50.2	72.3
2	449	5.38	491	0.78	1.1	1.1	12200	85.7	142.4

[a] Concentrations of 1×10^{-6} M and 1×10^{-4} M for the 1PA- and 2PA-related measurements, respectively. [b] One-photon absorption maximum. [c] Molar absorption coefficient. [d] 1PA-induced fluorescence emission maximum. [e] Fluorescence quantum efficiency. [f] 1PA-induced fluorescence lifetime, approximate value. [g] 2PA-induced fluorescence lifetime, approximate value. [h] Maximum 2PA cross-section (experimental error: about $\pm 15\%$); 1 GM = 1×10^{-50} cm⁴s/photon-molecule. [i] Effective π -electron number.^[18]

process. The experimental 1PA/2PA-induced fluorescence lifetimes for solutions of each model compound are listed in Table 1.

2.2. Degenerate Two-Photon-Absorption Spectroscopy

By using the aforementioned femtosecond laser system as the probing tool, the distribution in 2PA activities of the studied dye molecules was mapped out as a function of wavelength within the spectral region of 680–1000 nm by using the degenerate two-photon-excited fluorescence (2PEF) technique; an 80 μ M solution of fluorescein in NaOH (pH 11) was used as the standard for these experiments.^[16,17] Figure 5 shows the experimental degenerate two-photon-absorption spectra of these two model compounds in toluene (concentration: 1×10^{-4} M) and the combined photophysical data are summarized in Table 1. Notably, all of the studied compounds exhibit strong 2PA ($\delta_2 \geq 500$ GM) within the spectroscopic range 700–870 nm. Moreover, both of these model chromophores also possess a local 2PA maximum at around 800 nm, with 2PA cross-section values of about 3630 GM for compound **1** and 12200 GM for compound **2**.

3. Discussion

There are several notable features of the photophysical properties of the studied compounds in this work: 1) Based on the observed linear absorptions and 2PA behavior of these chromophores and by using compound **1** as a reference material for comparison, compound **2** exhibited saliently promoted linear absorption and 2PA, whilst retaining almost identical shapes and spectroscopic positions to those of compound **1**. These results indicate that excitonic coupling between branches of compound **2** seems to be effectively blocked so that only hyperchromic enhancement on both one-photon and two-photon absorp-

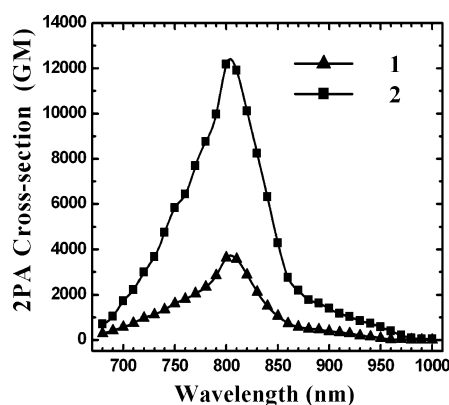


Figure 5. Experimental degenerate two-photon-absorption spectra of the studied model chromophores by using the 2PEF method at a concentration of 1×10^{-4} M in toluene (experimental error: about $\pm 15\%$).

tivities can be observed. This feature could be useful for molecular design when large 2PA values within a specific spectroscopic range are required for various applications. In addition, the observed solvatochromic behavior from chromophore **2** (Figure 3) suggests that the relaxed excited state of this model compound is highly dipolar and is sensitive to the polarity of environment. 2) Chromophore **2** exhibited a maximum 2PA cross-section that was slightly more than three times that of compound **1** (i.e., $\delta_2^{\max}(\mathbf{2})/\delta_2^{\max}(\mathbf{1}) \approx 3.36$), which indicated that enlarging the size of the molecule, which was accomplished by attaching two more identical 2,3,8-trisubstituted indenoquinoline branches onto the central triphenylamine core, only provided linearly promoted molecular 2PA. That is, we can assume that the large overall 2PA for compound **2** is inherited from compound **1** and, perhaps, the structure–property analysis should be focused on the parameters that lead to the strong 2PA of compound **1**. From the viewpoint of the molecular structure of chromophore **1**, the arrangement of the π units in this compound may permit unsymmetrical charge transfer/redistribution between the molecular termini and the central heterocyclic ring complex under the excitation of light because this π system utilizes an electron-deficient fused pyrazine ring to combine various peripheral electron-donating moieties with uneven electron-pushing strengths within one molecule. Although at this stage, there is no clear understanding of how this type of structural arrangement is related to the molecular two-photon activities, our preliminary results show that such structural combination may help to promote the molecular 2PA. Moreover, the maximum two-photon-absorption cross-sections of these two model compounds are comparable to those of reported 2PA chromophores that have similar effective π -electron numbers.^[18] 3) Because the observed fluorescence emission spectra (Figure 2 and Figure 4) and fluorescence lifetimes (Table 1 and the Supporting Information, Figure S3) are almost identical for one- and two-photon excitations for each individual model compound, we may conclude that, in these cases, the fluorescence emission predominantly origi-

nates from the same singlet state of each model chromophore and is independent of the excitation process.^[19]

4. Effective Optical-Power-Limiting Performance in the Nanosecond Regime

An ideal optical limiter is expected to show an intensity-dependent transmission feature so that it can act as a transparent medium when the incident intensity of light stays low and, once the input intensity increases, the medium starts to regulate the transmitted output intensity to be always below a certain maximum value before any optical saturation or damage occurs. This feature makes optical limiters not only useful for the protection of human eyes and sensors against hazardous light sources but it is also important for the compression of the optical dynamic range and noise suppression in signal processing, as well as the nonlinear ultrafast filtering/reshaping of signals from optical fibers.

Recently, it has been pointed out that the intensity-dependent 2PA-induced excited-state absorption (2PA-induced ESA) plays an essential role in the observed large 2PA in various organic systems under the irradiation of nanosecond laser pulses.^[20] From an application standpoint, any medium that possesses a large apparent nonlinear absorption covering a wide spectroscopic range could be very useful for optical-power attenuators against long laser pulses.^[21]

We have utilized nanosecond laser pulses to demonstrate the effective power-limiting performance of these model compounds. In our experiment, the nonlinear absorbing medium was a 1 cm path-length solution of the studied dye in toluene at a concentration of 0.01 M. A tunable nanosecond laser system (integrated Q-switched Nd:YAG laser and OPO:NT 342/3, Ekspla) was employed as an excitation laser light source to provide laser pulses (about 6 ns) with controlled average pulse energy within the range 0.02–2 mJ and a repetition rate of 10 Hz. The laser beam was slightly focused onto the center of the sample solution to create an almost-uniform laser-beam radius within the whole light path length and the transmitted laser beam from the sample solution was detected by using an optical power (energy) meter with a large detection area (diameter ≈ 25 mm). Figure 6 shows the power-attenuation performance at 800 nm, based on these chromophore solutions. Compound **2** shows superior power-restriction properties at 800 nm compared to compound **1**, which suggests the potential of using this model fluorophore as a candidate for broadband power-control-related applications within the nanosecond regime.

In addition, the output/input curve, as shown in Figure 6, shows a characteristic type of optical compression, which is ideal for use in optical-power (or optical-intensity) stabilization because a huge magnitude change in the input signal would only lead to a small variation in the output level,^[22] which means that a larger fluctuation in input power (or intensity) would practically lead to a much-smaller fluctuation in the output by passing through a nonlinear absorptive medium, such as the solution of model chromophore **2**. The

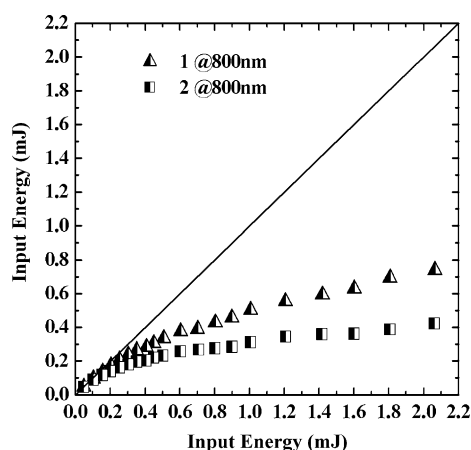


Figure 6. Experimental optical-power-attenuation curve based on the sample solution of compound **2** under the excitation of nanosecond laser pulses at 800 nm.

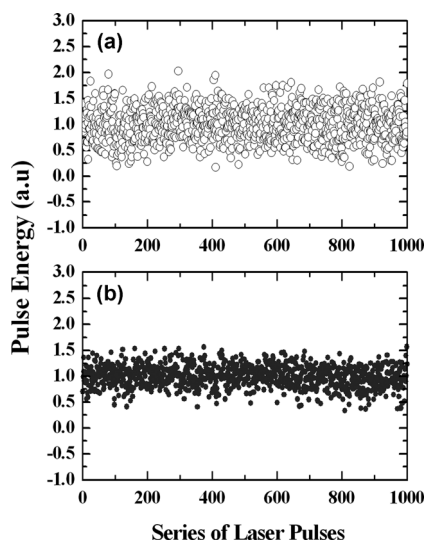


Figure 7. a) Experimental instantaneous pulse-energy fluctuation of the input laser pulses and b) experimental instantaneous pulse-energy fluctuation of the output laser pulses. The repetition rate of the laser pulses was 10 Hz and the average input pulse-energy level was about 0.8 mJ.

experimental results from an optical-stabilization study based on the same sample solutions are shown in Figure 7. The curves in Figure 7a,b show the instantaneous pulse-energy changes in the input and output laser pulses at 800 nm. For the purpose of comparison, the average levels of both the input and output signals were normalized to the same value. Clearly, the input pulses possess a relatively larger energy fluctuation (Figure 7a) and, after passing through the solution of compound **2**, a smaller fluctuation in pulse energy is observed for the output signal (Figure 7b).

Notably, the individual contributions of 2PA and ESA to the observed optical attenuation of the studied chromophore system are indistinguishable under our current experimental conditions. Nevertheless, it is very important for material chemists in this research field to gain insight into how

these processes relate to the molecular structures, in particular the effect of ESA in optimizing the materials on the molecular level for optical-control-related applications. Several attempts have been made to map out the dispersion of 2PA-assisted ESA by using pump-probe experiments^[20a,23] and such experiments are one of the major subjects of our future work.

Conclusions

We have characterized the degenerate two-photon-absorption-related properties of a new set of model chromophores with multi-branched molecular structures that were based on tri-substituted indenoquinoxaline skeletons, both in the femtosecond and nanosecond regimes, by using two-photon-excited fluorescence and nonlinear transmission techniques as the probing tools. We demonstrated that a chromophore that was derived from a multi-substituted quinoxalinoind ring complex with electron-donating units, which manifested uneven electron-pushing strengths, possessed strong molecular 2PA within a specific spectroscopic region. Moreover, increasing the branch number provided an efficient way of promoting molecular 2PA without shifting the major 2PA band. We also observed that model compound **2** exhibited both intense upconverted emission when excited by a two-photon process and effective optical-power limiting/stabilization against nanosecond laser pulses. These features make this chromophore a potential candidate as an efficient frequency upconverter and/or optical-power attenuator for various photonic applications.

Experimental Section

General

All commercially available reagents for the preparation of the intermediates and target chromophores were purchased from Aldrich Chemical Co. or Alfa Aesar and were used as received, unless otherwise stated. ¹H NMR and ¹³C NMR spectra were recorded on a 300 MHz spectrometer and referenced to tetramethylsilane (TMS) or to residual CHCl₃. The representative atom-numbering of the carbon and hydrogen atoms on each intermediate and model chromophore for the NMR assignment is shown in the Supporting Information, Figure S1. High-resolution mass spectroscopy (HRMS) was performed on a Waters LCT ESI-TOF mass spectrometer. MALDI-TOF mass spectra were recorded on a Voyager DE-PRO mass spectrometer (Applied Biosystem, Houston, USA).

Photophysical Methods

The linear optical properties of the model compound were measured on their corresponding spectrometers and the detailed experimental conditions, as well as the optical setups, for the investigation of nonlinear optical properties are described in the Supporting Information.

Synthesis

Compound **3** and **4** (Scheme 1) are the major starting materials for the synthesis of the backbones in each intermediate and model chromophore. These two compounds were obtained by following literature procedures^[9a] from 2,7-dibromofluorene as the starting material through alkylation at C9 position of the fluorene unit (to afford compound **3**), followed by Buchwald-type amination to afford compound **4** in about 80% and 50%

yield, respectively. For the syntheses of other key intermediates (compounds **6–12**) and the target model compounds (**1** and **2**), a series of functionalization steps from compounds **3** and **4** were performed, as presented below.

7-(2-(7-(Diphenylamino)-9,9-dihexyl-9H-fluoren-2-yl)ethynyl-9,9-dihexyl-N,N-diphenyl-9H-fluoren-2-amine (5)

To a three-necked round-bottomed flask (250 mL) were added compound **4** (5.13 g, 8.84 mmol), acetylenedicarboxylic acid (0.50 g, 4.42 mmol), [Pd(PPh₃)₂Cl₂] (0.03 g, 0.04 mmol), 1,4-bis(diphenylphosphino)butane > (DPPB, 0.37 g, 0.88 mmol), 1,8-diazabicyclo[5.4.0]undec-7-ene (DBU, 2.26 mL), and DMSO (20.5 mL) and the reaction mixture was stirred at 110°C under a N₂ atmosphere for 8 h. After cooling to RT, MeOH (10 mL) and cold hexanes (10 mL) were added to the reaction mixture, which was stirred at 0°C for 20 min. After filtration, the crude product was washed with MeOH and the final product was obtained as yellow powder (3.31 g, 73% yield). ¹H NMR (300 MHz, CDCl₃): δ = 7.60–7.45 (m, 8H; H₉, H₁₂, H₁₃, H₁₅), 7.28–7.19 (m, 10H; H₃, H₈), 7.13–7.07 (m, 10H; H₂, H₆), 7.03–6.97 (m, 4H; H₁), 1.95–1.83 (m, 8H; H₇), 1.16–1.06 (m, 24H; H_c, H_d, H_e), 0.82–0.77 (m, 12H; H_a), 0.66 ppm (m, 8H; H_b); ¹³C NMR (75 MHz, CDCl₃): δ = 152.47 (C₅), 150.67 (C₁₆), 147.92 (C₄), 147.54 (C₇), 141.12 (C₁₁), 135.56 (C₁₀), 130.63 (C₁₅), 129.17 (C₂), 125.73 (C₁₃), 123.91 (C₃), 123.45 (C₉), 122.61 (C₁), 120.77 (C₁₂), 120.65 (C₆), 119.09 (C₈), 119.02 (C₁₄), 90.51 (sp C atoms), 55.10 (C_g), 40.29 (C_i), 31.55 (C_e), 29.64 (C_d), 23.76 (C_c), 22.56 (C_b), 14.01 ppm (C_a); HRMS (FAB): *m/z* calcd for C₇₆H₈₄N₂: 1024.6635 [M]⁺; found: 1024.6639.

1,2-bis(7-(Diphenylamino)-9,9-dihexyl-9H-fluoren-2-yl)ethane-1,2-dione (6)

To a solution of compound **5** (3.31 g, 3.23 mmol) in CH₂Cl₂ (10.9 mL) were added KMnO₄ (2.04 g, 0.01 mol), NaHCO₃ (0.27 g, 3.23 mmol), Aliquat 336 (0.13 g), and water (10.9 mL) and the resulting solution was stirred at RT for 12 h. After the reaction was complete, a saturated aqueous solution of NaHCO₃ (30 mL) and a 1 M aqueous solution of HCl (30 mL) was added to the mixture. The mixed solution was extracted with CH₂Cl₂ (3 × 50 mL) and the organic layer was collected and dried over MgSO₄. After filtration and removal of the solvent, the crude product was purified by column chromatography on silica gel (CH₂Cl₂/hexanes, 1:3) to give the final product as a red powder (2.43 g, 71% yield). ¹H NMR (300 MHz, CDCl₃): δ = 8.03 (s, 2H; H₁₅), 7.88–7.84 (d, *J* = 9 Hz, 2H; H₁₃), 7.65–7.62 (d, *J* = 9 Hz, 2H; H₁₂), 7.60–7.58 (d, *J* = 6 Hz; H₉), 7.29–7.24 (m, 8H; H₃), 7.14–7.10 (m, 10H; H₂, H₆), 7.07–7.01 (m, 6H; H₁, H₈), 2.04–1.78 (m, 8H; H₇), 1.15–1.05 (m, 24H; H_c, H_d, H_e), 0.82–0.77 (m, 12H; H_a), 0.64 ppm (m, 8H; H_b); ¹³C NMR (75 MHz, CDCl₃): δ = 195.13 (C=O), 153.86 (C₅), 151.29 (C₁₆), 149.05 (C₁₁), 147.77 (C₇), 147.59 (C₄), 133.82 (C₁₄), 130.98 (C₁₀), 130.84 (C₁₅), 129.28 (C₂), 124.44 (C₃), 123.17 (C₁), 122.74 (C₁₂), 121.81 (C₉, C₁₃), 118.85 (C₆), 118.09 (C₈), 55.29 (C_g), 39.91 (C_i), 31.44 (C_e), 29.48 (C_d), 23.75 (C_c), 22.49 (C_b), 13.98 ppm (C_a); HRMS (FAB): *m/z* calcd for C₇₆H₈₄N₂O₂: 1056.6533 [M]⁺; found: 1056.6627.

7-Bromo-9,9-dihexyl-9H-fluoren-2-amine (7)

Step 1: To a three-necked round-bottom flask (250 mL) were added compound **3** (7.42 g, 0.01 mol), potassium phthalimide (2.77 g, 0.01 mol), CuI (2.87 g, 0.01 mol), and DMAc (148 mL) and the reaction solution was stirred at 165°C for 48 h. After cooling to RT, the reaction mixture was quenched with aqueous ammonia to scavenge the excess CuI. Then, the solution was extracted with EtOAc (3 × 100 mL) and the organic layer was collected and dried over MgSO₄. After filtration and removal of the solvent, the crude product was purified by column chromatography on silica gel (EtOAc/hexanes, 1:10) to give the final product as a brown oil (4.63 g, 55% yield). ¹H NMR (300 MHz, CDCl₃): δ = 8.00–7.97 (dd, ¹*J* = 5.4 Hz, ²*J* = 3.3 Hz, 2H; ArH of the phthalimide unit), 7.83–7.78 (m, 3H; H₁ and ArH of the phthalimide unit), 7.62–7.59 (m, 1H; H_E), 7.51–7.50 (m, 2H; H_H, H_K), 7.48–7.47 (m, 1H; H_D), 7.44 (s, 1H; H_B), 1.99–1.94 (m, 4H; H_F), 1.30–1.09 (m, 12H; H_c, H_d, H_e), 0.82–0.68 ppm (m, 10H; H_a, H_b); ¹³C NMR (75 MHz, CDCl₃): δ = 167.28 (C=O of the phthalimide unit), 153.39 (C_A), 151.05 (C_L), 139.57 (C_C), 139.23 (C_F), 134.36 (benzene

ring of the phthalimide unit), 131.78 (C_N), 130.82 (C_B), 130.09 (C_J), 126.23 (C_I), 125.13 (C_D), 123.63 (benzene ring of the phthalimide unit), 121.27 (C_K), 121.21 (C_H), 120.07 (C_C, C_E), 55.62 (C_G), 40.06 (C_F), 31.40 (C_e), 29.60 (C_d), 23.73 (C_c), 22.52 (C_b), 13.94 ppm (C_a).

Step 2: To a solution of the product from the first step (4.63 g, 8.31 mmol) in MeOH (65.3 mL) was slowly added hydrazine monohydrate (0.41 g, 8.31 mmol) and the mixture was stirred at 80°C for 6 h. After cooling to RT, the reaction solution was extracted with EtOAc (3 × 50 mL) and the organic layer was collected and dried over MgSO₄. After filtration and removal of the solvent, the crude product was purified by column chromatography on silica gel (EtOAc/hexanes, 1:25) to give the final product as a brown oil (3.24 g, 91% yield). ¹H NMR (300 MHz, CDCl₃): δ = 7.39–7.32 (m, 4H; H_B, H_D, H_E, H_H), 6.55–6.51 (m, 2H; H_I, H_K), 3.62 (s, 1H; N_H), 1.87–1.84 (m, 4H; H_F), 1.12–1.01 (m, 12H; H_c, H_d, H_e), 0.75–0.61 ppm (m, 10H; H_a, H_b); ¹³C NMR (75 MHz, CDCl₃): δ = 151.88 (C_A), 151.81 (C_L), 140.43 (C_F), 130.69 (C_G), 129.42 (C_B), 125.51 (C_D), 120.38 (C_E), 119.35 (C_H), 119.72 (C_C), 113.73 (C_K), 109.12 (C_I), 54.80 (C_G), 40.29 (C_F), 31.24 (C_e), 29.47 (C_d), 23.42 (C_c), 22.37 (C_b), 13.80 ppm (C_a); HRMS (FAB): *m/z* calcd for C₂₅H₃₄BrN: 428.4482 [M+H]⁺; found: 428.4361.

N-(7-Bromo-9,9-dihexyl-9H-fluoren-2-yl)acetamide (8)

A mixture of compound **7** (3.24 g, 7.58 mmol), triethylamine (1.26 mL, 9.10 mol), and acetic anhydride (0.82 g, 9.10 mol) in CH₂Cl₂ (32.4 mL) was stirred at 30°C for 4 h. After cooling to RT, the solution was extracted with EtOAc (3 × 50 mL) and the organic layer was dried over MgSO₄. After filtration and removal of the solvent, the compound was obtained as a white solid (3.39 g, 95% yield). ¹H NMR (300 MHz, CDCl₃): δ = 7.63–7.53 (m, 2H; N_H, H_E), 7.50–7.42 (m, 4H; H_B, H_D, H_H, H_K), 7.38–7.32 (m, 1H; H_I), 2.21 (s, 3H; CH₃ atoms of the acetyl group), 1.94–1.88 (m, 4H; H_F), 1.14–1.03 (m, 12H; H_c, H_d, H_e), 0.79–0.74 (m, 6H; H_a), 0.61–0.59 ppm (m, 4H; H_b); ¹³C NMR (75 MHz, CDCl₃): δ = 168.27 (C=O of the acetyl group), 152.82 (C_L), 151.46 (C_A), 139.68 (C_G), 137.63 (C_F), 136.19 (C_J), 135.75 (C_H), 129.86 (C_B), 126.00 (C_D), 120.56 (C_E), 120.06 (C_C), 118.52 (C_K), 114.26 (C_I), 55.48 (C_G), 40.25 (C_F), 31.43 (C_e), 29.58 (C_d), 24.66 (CH₃ atom of the acetyl group), 23.64 (C_c), 22.51 (C_b), 13.92 ppm (C_a); HRMS (FAB): *m/z* calcd for C₂₇H₃₆BrNO: 469.1980 [M]⁺; found: 469.1980.

N-(7-Bromo-9,9-dihexyl-3-nitro-9H-fluoren-2-yl)acetamide (9)

A solution of compound **8** (3.39 g, 7.22 mmol) in acetic acid (50.8 mL) and acetone (16.9 mL) was stirred for 5–10 min and then fuming HNO₃ (2.43 mL; 0.06 mol) was added dropwise at 0–5°C. After the reaction had finished (by TLC), the reaction mixture was extracted with EtOAc (3 × 50 mL) and the organic layer was dried over MgSO₄. After filtration and removal of the solvent, the crude product was purified by column chromatography on silica gel (EtOAc/hexanes, 1:10) to give the final product as a yellow powder (2.98 g, 80% yield). ¹H NMR (300 MHz, CDCl₃): δ = 10.59 (s, 1H; NH), 8.81 (s, 1H; H_H), 8.47 (s, 1H; H_K), 7.71–7.44 (m, 3H; H_B, H_D, H_E), 2.32 (s, 1H; CH₃ atoms of the acetyl group), 2.02–1.97 (m, 4H; H_F), 1.12–1.05 (m, 12H; H_c, H_d, H_e), 0.78–0.73 (m, 6H; H_a), 0.61–0.59 ppm (m, 4H; H_b); ¹³C NMR (75 MHz, CDCl₃): δ = 168.92 (C=O of the acetyl group), 159.27 (C_L), 152.68 (C_A), 137.45 (C_F), 136.48 (C_J), 135.71 (C_G), 134.61 (C_I), 130.51 (C_B), 126.32 (C_D), 122.30 (C_E), 121.29 (C_C), 116.51 (C_H), 116.10 (C_K), 56.44 (C_G), 40.05 (C_F), 31.29 (C_e), 29.37 (C_d), 25.68 (CH₃ of the acetyl group), 23.67 (C_c), 22.40 (C_b), 13.83 ppm (C_a); HRMS (FAB): *m/z* calcd for C₂₇H₃₅BrN₂O₃: 514.1831 [M]⁺; found: 514.1837.

7-Bromo-9,9-dihexyl-3-nitro-9H-fluoren-2-amine (10)

To a solution of compound **9** (2.98 g, 5.78 mmol) in MeOH (47.2 mL) was slowly added H₂SO₄ (8.10 mL) and the solution was stirred at reflux for 10 h. After cooling to RT, the solution was extracted with EtOAc (3 × 30 mL) and the organic layer was dried over MgSO₄. After filtration and removal of the solvent, the crude product was purified by column chromatography on silica gel (EtOAc/hexanes, 1:10) to give the final product as a red solid (2.73 g, 93% yield). ¹H NMR (300 MHz, CDCl₃): δ = 8.37 (s, 1H; H_H), 7.64–7.36 (m, 3H; H_C, H_D, H_E), 6.72 (s, 1H; H_K), 6.26 (s,

2H; NH₂), 1.96–1.79 (m, 4H; H_F), 1.16–1.04 (m, 12H; H_C, H_d, H_E), 0.79–0.75 (m, 6H; H_a), 0.63–0.58 ppm (m, 4H; H_b); ¹³C NMR (75 MHz, CDCl₃): δ = 159.52 (C_L), 151.43 (C_A), 144.97 (C_J), 138.31 (C_F), 136.31 (C_G), 130.44 (C_I), 126.04 (C_E, C_D), 121.01 (C_H), 120.72 (C_C), 116.77 (C_B), 112.33 (C_K), 55.62 (C_G), 40.76 (C_F), 31.39 (C_E), 29.52 (C_d), 23.72 (C_c), 22.49 (C_b), 13.90 ppm (C_a); HRMS (FAB): *m/z* calcd for C₂₅H₃₃BrN₂O₂: 472.1725 [M]⁺; found: 472.1722.

7-Bromo-9,9-dihexyl-9H-fluoren-2,3-diamine (11)

To a mixture of compound **10** (2.00 g, 4.23 mmol) and stannous chloride (9.55 g, 0.04 mol) was added EtOAc (41.5 mL) and the reaction solution was stirred at 80 °C for 4 h. After the reaction had finished, the mixture was quenched with an aqueous solution of NaHCO₃. This solution was extracted with EtOAc (3 × 50 mL) and the organic layer was dried over MgSO₄. After removal of the solvent, the crude product was purified by column chromatography on silica gel (EtOAc/hexanes, 1:3) to give the final product as a yellow powder (1.33 g, 71% yield). ¹H NMR (300 MHz, CDCl₃): δ = 7.37–7.36 (d, *J* = 1.5 Hz, 1H; H_B), 7.35–7.32 (dd, ¹*J* = 7.8 Hz, ¹*J* = 1.5 Hz, 1H; H_D), 7.27–7.25 (d, *J* = 7.8 Hz, 1H; H_E), 6.92 (s, 1H; H_K), 6.60 (s, 1H; H_H), 3.44 (s, 4H; NH₂), 1.85–1.80 (m, 4H; H_F), 1.03–1.01 (m, 12H; H_C, H_d, H_E), 0.77–0.72 (t, *J* = 7.2 Hz, 6H; H_a), 0.64–0.62 ppm (m, 4H; H_b); ¹³C NMR (75 MHz, CDCl₃): δ = 152.59 (C_A), 142.93 (C_L), 140.62 (C_F), 135.19 (C_J), 133.41 (C_I), 132.02 (C_E), 129.37 (C_D), 125.50 (C_B), 119.39 (C_G), 118.82 (C_C), 110.62 (C_H), 108.08 (C_K), 54.52 (C_G), 40.32 (C_F), 31.34 (C_E), 29.55 (C_d), 23.52 (C_c), 22.44 (C_b), 13.85 ppm (C_a).

7,7-(8-Bromo-10,10-dihexyl-10H-indeno[1,2g]quinoxaline-2,3-diyl)bis(9,9-dihexyl-*N,N*-diphenyl-9H-fluoren-2-amine) (12)

To a mixture of compound **11** (1.22 g, 2.76 mmol) and compound **6** (2.43 g, 2.30 mmol) was added acetic acid (30.5 mL) and THF (4.05 mL) and the reaction solution was stirred at 110 °C under a N₂ atmosphere for 12 h. After cooling to RT, the solution was extracted with EtOAc (3 × 150 mL) and the organic layer was dried over MgSO₄. After filtration and removal of the solvent, the crude product was purified by column chromatography on silica gel (CH₂Cl₂/hexanes, 1:5) to give the final product as a yellow solid (3.00 g, 89% yield). ¹H NMR (300 MHz, CDCl₃): δ = 8.45 (s, 1H; H_H), 8.11 (s, 1H; H_K), 7.82–7.80 (d, 1H, *J* = 8.1 Hz; H_D), 7.58–7.55 (m, 10H; H₉, H₁₂, H₁₃, H₁₅, H_B, H_E), 7.30–7.25 (m, 8H; H₂), 7.16–7.12 (m, 10H; H₃, H₆), 7.04 (m, 6H, H₁, H₈), 2.20–2.12 (m, 4H; H_F), 1.78–1.68 (m, 8H; H_F), 1.29–0.89 (m, 36H; H_a, H_d, H_e, H_c, H_d, H_e), 0.84–0.69 ppm (m, 30H; H_a, H_b, H_a, H_b); ¹³C NMR (75 MHz, CDCl₃): δ = 153.49 (C₁₆), 153.07 (C₁₇), 152.84 (C₁₈), 152.58 (C₃), 150.58 (C_A), 150.50 (C_G), 147.90 (C₄), 147.40 (C₇), 142.79 (C_F), 141.28 (C_J), 141.18 (C_I), 138.69 (C₁₁), 137.47 (C_K), 137.41 (C_H), 135.52 (C₁₀), 130.59 (C₁₄), 129.11 (C₂, C₁₅), 126.70 (C₁₂), 124.35 (C₁₃), 123.83 (C₅), 123.37 (C₉), 122.51 (C₁), 122.37 (C_B), 120.81 (C_D), 119.09 (C₆), 118.93 (C₈), 118.44 (C_C), 55.47 (C_G), 55.04 (C_G), 41.27 (C_F), 40.09 (C_I), 31.52 (C_e, C_e), 29.63 (C_d), 29.57 (C_d), 23.83 (C_c, C_c), 22.59 (C_b), 22.53 (C_b), 14.05 (C_a), 13.92 ppm (C_a); HRMS (MALDI-TOF): *m/z* calcd for C₁₀₁H₁₁₅BrN₄ (theoretical average): 1463.8305 [M+H]⁺; found: 1463.8384.

Compound 1

A solution of compound **12** (1.0 g, 0.68 mmol), (4-vinylphenyl)amine (0.20 g, 0.75 mmol), Pd(OAc)₂ (3.06 mg, 0.013 mmol), and tri(*o*-totyl)phosphine (0.025 g, 0.082 mmol) in MeCN (8 mL) and NEt₃ (4 mL) was prepared in a heavy-walled tube (ACE Glass). The reaction mixture was sealed and stirred at 110 °C under a N₂ atmosphere for 72 h. After cooling to RT, the resulting solution was extracted with CH₂Cl₂ (3 × 50 mL) and the organic layer was dried over MgSO₄. After filtration and removal of the solvent, the crude product was purified by column chromatography on silica gel (EtOAc/hexanes, 1:40) to give the final product as a yellow powder in (0.77 g, 83% yield). ¹H NMR (300 MHz, CDCl₃): δ = 8.41 (s, 1H; H_H), 8.08 (s, 1H; H_K), 7.90–7.87 (d, *J* = 7.8 Hz, 1H; H_D), 7.59–7.43 (m, 11H; H₉, H₁₂, H₁₃, H₁₅, H_B, H_E, H_D), 7.26–7.21 (m, 13H; H₂, H_A, H_F), 7.13–7.06 (m, 18H; H₃, H₆, H_D, H_E, H_H), 7.02–7.00 (m, 8H; H₁, H₈, H_J), 2.11 (m, 4H; H_F), 1.75–1.66 (m, 8H; H_F), 1.11–1.05 (m, 36H; H_a, H_d, H_e, H_c, H_d, H_e), 0.81–0.69 ppm (m, 30H; H_a, H_b, H_a, H_b); ¹³C NMR

(75 MHz, CDCl₃): δ = 153.81 (C₅), 153.27 (C₁₇), 152.60 (C₁₈), 151.93 (C₁₆), 150.56 (C_A, C_B), 147.93 (C₄, C_G), 147.49 (C₁₁), 147.37 (C_F), 143.79 (C₆), 141.40 (C_I, C_J), 141.23 (C_J), 139.04 (C_C), 138.53 (C₈), 137.68 (C_K), 137.61 (C_H), 135.62 (C₁₀), 131.40 (C_D), 129.27 (C_I), 129.12 (C₂), 128.44 (C_C), 127.40 (C_B), 127.30 (C_A), 125.83 (C₁₃), 124.55 (C₁₄), 124.40 (C_E), 123.83 (C₃, C_H), 123.45 (C₁₃), 123.08 (C_E), 122.50 (C₁, C_J), 122.18 (C_B), 121.31 (C_D), 120.79 (C₆), 119.16 (C₉), 118.92 (C₈), 117.89 (C₁₂), 55.05 (C_G), 41.44 (C_F), 40.11 (C_I), 31.54 (C_e, C_e), 29.73 (C_d), 29.59 (C_d), 23.85 (C_c, C_c), 22.60 (C_b, C_b), 14.06 (C_a), 13.94 ppm (C_a); HRMS (FAB): *m/z* calcd for C₁₂₁H₁₃₁N₅: 1564.0404 [M]⁺; found: 1654.0413.

Compound 2

A solution of compound **12** (1.0 g, 0.68 mmol), tris(4-vinylphenyl)amine (0.067 g, 0.21 mmol), Pd(OAc)₂ (2.78 mg, 0.012 mmol), and tri(*o*-totyl)phosphine (0.023 g, 0.074 mmol) in MeCN (8 mL) and NEt₃ (4 mL) was prepared in a heavy-walled tube (ACE Glass). The reaction mixture was stirred at 110 °C under a N₂ atmosphere for 72 h. After cooling to RT, the solution was extracted with CH₂Cl₂ (3 × 50 mL) and the organic layer was dried over MgSO₄. After filtration and removal of the solvent, the crude product was purified by column chromatography on silica gel (THF/hexanes, 1:15) to give the final product as a yellow solid (1.00 g, 80% yield). ¹H NMR (300 MHz, CDCl₃): δ = 8.41 (s, 3H; H_H), 8.09 (s, 3H; H_K), 7.92–7.89 (d, *J* = 7.8 Hz, 3H; H_D), 7.59–7.52 (m, 36H; H₉, H₁₂, H₁₃, H₁₅, H_A, H_B, H_B, H_E), 7.27–7.18 (m, 36H; H₂, H_D, H_E), 7.13–7.08 (m, 30H; H₃, H₆), 7.03–6.99 (m, 8H; H₁, H₈), 2.15 (m, 4H; H_F), 1.74 (m, 8H; H_F), 1.11–1.05 (m, 36H; H_a, H_d, H_e, H_c, H_d, H_e), 0.81–0.74 ppm (m, 30H; H_a, H_b, H_a, H_b); ¹³C NMR (75 MHz, CDCl₃): δ = 153.82 (C₅), 153.33 (C₁₇), 152.71 (C₁₈), 152.63 (C₁₆), 152.00 (C₁₈), 150.59 (C₇), 150.54 (C₁₂), 147.95 (C₄), 147.40 (C₁₁), 146.78 (C_F), 143.78 (C_G), 141.45 (C_I, C_J), 141.28 (C_J), 139.22 (C_C), 138.42 (C₈), 137.67 (C_H), 137.61 (C_K), 135.64 (C₁₀), 132.31 (C_D), 129.14 (C₂), 128.31 (C_C), 127.59 (C_A, C_B), 125.94 (C₁₃), 124.41 (C₁₄, C_E), 123.85 (C_D), 123.43 (C₁₃), 122.53 (C₁), 122.24 (C_B), 121.39 (C_D), 120.83 (C₆), 119.18 (C₉), 118.95 (C₈), 117.97 (C₁₂), 55.08 (C_G), 41.47 (C_F), 40.03 (C_I), 31.56 (C_e, C_e), 29.77 (C_d), 29.61 (C_d), 23.87 (C_c, C_c), 22.62 (C_b, C_b), 14.08 (C_a), 13.97 ppm (C_a); HRMS (MALDI-TOF): *m/z* calcd for C₃₂₇H₃₆₃N₁₃ (theoretical average): 4476.5986 [M+1H]⁺; found: 4476.6123.

Acknowledgements

We acknowledge financial support from the National Science Council (NSC), Taiwan, (101-2113M-008-003-MY2). F.L.G. also acknowledges the great help from Ms. Ying-Hsuan Lee with the synthesis work.

- [1] M. Göppert-Mayer, *Ann. Phys.* **1931**, *401*, 273–295.
- [2] W. Kaiser, C. G. B. Garret, *Phys. Rev. Lett.* **1961**, *7*, 229–231.
- [3] a) S. Yao, K. D. Belfield, *Eur. J. Org. Chem.* **2012**, 3199–3217; b) M. Pawlicki, H. A. Collins, R. G. Denning, H. L. Anderson, *Angew. Chem.* **2009**, *121*, 3292–3316; *Angew. Chem. Int. Ed.* **2009**, *48*, 3244–3266; c) M. Rumi, S. Barlow, J. Wang, J. W. Perry, S. R. Marder, *Adv. Polym. Sci.* **2008**, *213*, 1–95; d) K. D. Belfield, S. Yao, M. V. Bondar, *Adv. Polym. Sci.* **2008**, *213*, 97–156; e) C. W. Spangler, *J. Mater. Chem.* **1999**, *9*, 2013–2020; f) G. S. He, L.-S. Tan, Q. Zheng, P. N. Prasad, *Chem. Rev.* **2008**, *108*, 1245–1330; g) T.-C. Lin, S.-J. Chung, K.-S. Kim, X. Wang, G. S. He, J. Swiatkiewicz, H. E. Pudavar, P. N. Prasad, *Adv. Polym. Sci.* **2003**, *161*, 157–193.
- [4] For selected examples, see: a) M. Albota, D. Beljonne, J.-L. Brédas, J. E. Ehrlich, J.-Y. Fu, A. A. Heikal, S. E. Hess, T. Kogej, M. D. Levin, S. R. Marder, D. McCord-Maughon, J. W. Perry, H. Rockel, M. Rumi, G. Subramaniam, W. W. Webb, X.-L. Wu, C. Xu, *Science* **1998**, *281*, 1653–1656; b) M. Rumi, J. E. Ehrlich, A. A. Heikal, J. W. Perry, S. Barlow, Z. Hu, D. McCord-Maughon, T. C. Parker, H. Röel, S. Thayumanavan, S. R. Marder, D. Beljonne, J.-L. Brédas, *J. Am. Chem. Soc.* **2000**, *122*, 9500–9510.
- [5] For selected examples, see: a) O. Mongin, J. Brunel, L. Porrès, M. Blanchard-Desce, *Tetrahedron Lett.* **2003**, *44*, 2813–2816; b) O. Mongin, L. Porrès, C. Katan, T. Pons, J. Mertz, M. Blanchard-Desce,

- Tetrahedron Lett.* **2003**, *44*, 8121–8125; c) L. Porrès, C. Katan, O. Mongin, T. Pons, J. Mertz, M. Blanchard-Desce, *J. Mol. Struct.* **2004**, *704*, 17–24; d) L. Porrès, O. Mongin, C. Katan, M. Charlot, T. Pons, J. Mertz, M. Blanchard-Desce, *Org. Lett.* **2004**, *6*, 47–50; e) C. Katan, F. Terenziani, O. Mongin, M. H. V. Werts, L. Porrès, T. Pons, J. Mertz, S. Tretiak, M. Blanchard-Desce, *J. Phys. Chem. A* **2005**, *109*, 3024–3037; f) F. Terenziani, C. L. Droumaguet, C. Katan, O. Mongin, M. Blanchard-Desce, *ChemPhysChem* **2007**, *8*, 723–734; g) J. C. Collings, S.-Y. Poon, C. L. Droumaguet, M. Charlot, C. Katan, L.-O. Palsson, A. Beeby, J. A. Mosely, H. M. Kaiser, D. Kaufmann, W.-Y. Wong, M. Blanchard-Desce, T. B. Marder, *Chem. Eur. J.* **2009**, *15*, 198–208; h) F. Terenziani, V. Parthasarathy, A. Blanch-Quintana, T. Maishal, A.-M. Caminade, J.-P. Majoral, M. Blanchard-Desce, *Angew. Chem.* **2009**, *121*, 8847–8850; *Angew. Chem. Int. Ed.* **2009**, *48*, 8691–8694.
- [6] For selected examples, see: a) M. Drobizhev, A. Karotki, A. Rebane, C. W. Spangler, *Opt. Lett.* **2001**, *26*, 1081–1083; b) M. Drobizhev, A. Karotki, Y. Dzenis, A. Rebane, Z. Suo, C. W. Spangler, *J. Phys. Chem. B* **2003**, *107*, 7540–7543; c) M. Drobizhev, A. Rebane, Z. Suoc, C. W. Spangler, *J. Lumin.* **2005**, *111*, 291–305; d) M. Drobizhev, F. Meng, A. Rebane, Y. Stepanenko, E. Nickel, C. W. Spangler, *J. Phys. Chem. B* **2006**, *110*, 9802–9814.
- [7] For selected examples, see: a) K. D. Belfield, A. R. Morales, J. M. Hales, D. J. Hagan, E. W. V. Stryland, V. M. Chapela, J. Percino, *Chem. Mater.* **2004**, *16*, 2267–2273; b) K. D. Belfield, A. R. Morales, B.-S. Kang, J. M. Hales, D. J. Hagan, E. W. Van Stryland, V. M. Chapela, J. Percino, *Chem. Mater.* **2004**, *16*, 4634–4641; c) S. Yao, K. D. Belfield, *J. Org. Chem.* **2005**, *70*, 5126–5132; d) K. D. Belfield, M. V. Bondar, F. E. Hernandez, O. V. Przhonska, *J. Phys. Chem. C* **2008**, *112*, 5618–5622; e) X. Wang, D. M. Nguyen, C. O. Yanez, L. Rodriguez, H.-Y. Ahn, M. V. Bondar, K. D. Belfield, *J. Am. Chem. Soc.* **2010**, *132*, 12237–12239.
- [8] For selected examples, see: a) Y. Wang, G. S. He, P. N. Prasad, T. Goodson III., *J. Am. Chem. Soc.* **2005**, *127*, 10128–10129; b) A. Bhaskar, G. Ramakrishna, Z. Lu, R. Twieg, J. M. Hales, D. J. Hagan, E. V. Stryland, T. Goodson III., *J. Am. Chem. Soc.* **2006**, *128*, 11840–11849; c) A. Bhaskar, R. Guda, M. M. Haley, T. Goodson III., *J. Am. Chem. Soc.* **2006**, *128*, 13972–13973; d) O. Varnavski, X. Yan, O. Mongin, M. Blanchard-Desce, T. Goodson III., *J. Phys. Chem. C* **2007**, *111*, 149–162; e) M. Williams-Harry, A. Bhaskar, G. Ramakrishna, T. Goodson III., M. Imamura, A. Mawatari, K. Nakao, H. Enozawa, T. Nishinaga, M. Iyoda, *J. Am. Chem. Soc.* **2008**, *130*, 3252–3253.
- [9] For selected examples, see: a) B. A. Reinhardt, L. L. Brott, S. J. Clarson, A. G. Dillard, J. C. Bhatt, R. Kannan, L. Yuan, G. S. He, P. N. Prasad, *Chem. Mater.* **1998**, *10*, 1863–1874; b) R. Kannan, G. S. He, L. Yuan, F. Xu, P. N. Prasad, A. G. Dombroskie, B. A. Reinhardt, J. W. Baur, R. A. Vaia, L.-S. Tan, *Chem. Mater.* **2001**, *13*, 1896–1904; c) R. Kannan, G. S. He, T.-C. Lin, P. N. Prasad, R. A. Vaia, L.-S. Tan, *Chem. Mater.* **2004**, *16*, 185–194; d) S.-J. Chung, K.-S. Kim, T.-C. Lin, G. S. He, J. Swiatkiewicz, P. N. Prasad, *J. Phys. Chem. B* **1999**, *103*, 10741–10745; e) T.-C. Lin, G. S. He, P. N. Prasad, L.-S. Tan, *J. Mater. Chem.* **2004**, *14*, 982–991; f) Q. Zheng, G. S. He, P. N. Prasad, *Chem. Mater.* **2005**, *17*, 6004–6011.
- [10] For selected examples, see: a) H. J. Lee, J. Sohn, J. Hwang, S. Y. Park, H. Choi, M. Cha, *Chem. Mater.* **2004**, *16*, 456–465; b) Y.-Z. Cui, Q. Fang, G. Xue, G.-B. Xu, L. Yin, W.-T. Yu, *Chem. Lett.* **2005**, *34*, 644–645; c) J. Li, F. Meng, H. Tian, J. Mi, W. Ji, *Chem. Lett.* **2005**, *34*, 922–923; d) J. Wu, Y. Zhao, X. Li, M. Shi, F. Wu, X. Fang, *New J. Chem.* **2006**, *30*, 1098–1103.
- [11] For selected examples, see: a) T.-C. Lin, G. S. He, Q. Zheng, P. N. Prasad, *J. Mater. Chem.* **2006**, *16*, 2490–2498; b) T.-C. Lin, Y.-F. Chen, C.-L. Hu, C.-S. Hsu, *J. Mater. Chem.* **2009**, *19*, 7075–7080; c) T.-C. Lin, W.-L. Lin, C.-M. Wang, C.-W. Fu, *Eur. J. Org. Chem.* **2011**, 912–921; d) T.-C. Lin, Y.-H. Lee, C.-L. Hu, Y.-K. Li, Y.-J. Huang, *Eur. J. Org. Chem.* **2012**, 1737–1745; e) T.-C. Lin, Y.-H. Lee, B.-R. Huang, C.-L. Hu, Y.-K. Li, *Tetrahedron* **2012**, *68*, 4935–4949.
- [12] For selected examples, see: a) K. R. J. Thomas, J. T. Lin, Y.-T. Tao, C. H. Chuen, *J. Mater. Chem.* **2002**, *12*, 3516–3522; b) C.-T. Chen, J.-S. Lin, M. V. R. K. Moturn, Y.-W. Lin, W. Yi, Y.-T. Tao, C.-H. Chien, *Chem. Commun.* **2005**, 3980; c) K. R. J. Thomas, M. Velusamy, J. T. Lin, C.-H. Chuen, Y.-T. Tao, *Chem. Mater.* **2005**, *17*, 1860; d) A. P. Kulkarni, Y. Zhu, A. Babel, P.-T. Wu, S. A. Jenekhe, *Chem. Mater.* **2008**, *20*, 4212; e) D. Aldakov, M. A. Palacios, P. Anzenbacher, Jr., *Chem. Mater.* **2005**, *17*, 5238; f) F. S. Mancilha, B. A. D. Neto, A. S. Lopes, P. F. Moreira, Jr., F. H. Quina, R. S. Goncalves, J. Dupont, *Eur. J. Org. Chem.* **2006**, 4924; g) C.-T. Chen, Y. Wei, J.-S. Lin, M. V. R. K. Motoru, W.-S. Chao, Y.-T. Tao, C.-H. Chien, *J. Am. Chem. Soc.* **2006**, *128*, 10992.
- [13] a) H. Kishida, K. Hirota, T. Wakabayashi, B.-L. Lee, H. Kokubo, T. Yamamoto, H. Okamoto, *Phys. Rev. B* **2004**, *70*, 115205–115210; b) H. Kishida, K. Hirota, H. Okamoto, H. Kokubo, T. Yamamoto, *Synth. Met.* **2009**, *159*, 868–870; c) X. Cao, F. Jin, Y.-F. Li, W.-Q. Chen, X.-M. Duan, L.-M. Yang, *New J. Chem.* **2009**, *33*, 1578–1582.
- [14] K. Park, G. Bae, J. Moon, J. Choe, K. H. Song, S. Lee, *J. Org. Chem.* **2010**, *75*, 6244–6251.
- [15] a) M. Parent, O. Mongin, K. Kamada, C. Katan, M. Blanchard-Desce, *Chem. Commun.* **2005**, 2029–2031; b) C. Le Droumaguet, O. Mongin, M. H. V. Werts, M. Blanchard-Desce, *Chem. Commun.* **2005**, 2802–2804; c) F. Terenziani, A. Painelli, C. Katan, M. Charlot, M. Blanchard-Desce, *J. Am. Chem. Soc.* **2006**, *128*, 15742–15755; d) A. Painelli, F. Terenziani, Z. G. Soos, *Theor. Chem. Acc.* **2007**, *117*, 915–931.
- [16] C. Xu, W. W. Webb, *J. Opt. Soc. Am. B* **1996**, *13*, 481–491.
- [17] N. S. Makarov, M. Drobizhev, A. Rebane, *Opt. Express* **2008**, *16*, 4029–4047.
- [18] M. G. Kuzyk, *J. Chem. Phys.* **2003**, *119*, 8327–8334.
- [19] a) F. J. Duarte, L. W. Hillman, *Dye Laser Principles with Applications*, Academic Press, New York, **1990**; b) F. P. Schäfer, *Dye Lasers*, Springer, Berlin, **1990**.
- [20] a) R. L. Sutherland, M. C. Brant, J. Heinrichs, J. E. Rogers, J. E. Slagle, D. G. McLean, P. A. Fleitz, *J. Opt. Soc. Am. B* **2005**, *22*, 1939–1948; b) B. Gu, K. Lou, H.-T. Wang, W. Ji, *Opt. Lett.* **2010**, *35*, 417–419.
- [21] a) M. J. Miller, A. G. Mott, B. P. Ketchel, *Proc. SPIE* **1998**, *3472*, 24–29; b) J. S. Shirk, *Optics & Photonics News*, April **2000**, 19–23; c) J. Zhang, Y. Cui, M. Wang, J. Liu, *Chem. Commun.* **2002**, 2526–2527.
- [22] a) G. S. He, R. Gvishi, P. N. Prasad, B. A. Reinhardt, *Opt. Commun.* **1995**, *117*, 133–136; b) G. S. He, L. Yuan, N. Cheng, J. D. Bhawalkar, P. N. Prasad, L. L. Brott, S. J. Clarson, B. A. Reinhardt, *J. Opt. Soc. Am. B* **1997**, *14*, 1079–1087; c) G. S. He, C. Weder, P. Smith, P. N. Prasad, *IEEE J. Quantum Electron.* **1998**, *34*, 2279–2285; d) Q. Zheng, G. S. He, P. N. Prasad, *Chem. Phys. Lett.* **2009**, *475*, 250–255.
- [23] a) Y. Morel, A. Irimia, P. Najechalski, Y. Kervella, O. Stephan, P. L. Baldeck, C. Andraud, *J. Chem. Phys.* **2001**, *114*, 5391–5396; b) P.-A. Bouit, G. Wetzel, G. Berginc, B. Loiseaux, L. Toupet, P. Feneyrou, Y. Bretonnière, K. Kamada, O. Maury, C. Andraud, *Chem. Mater.* **2007**, *19*, 5325–5335; c) C. Li, K. Yang, Y. Feng, X. Su, J. Yang, X. Jin, M. Shui, Y. Wang, X. Zhang, Y. Song, H. Xu, *J. Phys. Chem. B* **2009**, *113*, 15730–15733; d) Q. Bellier, N. S. Makarov, P.-A. Bouit, S. Rigaut, K. Kamada, P. Feneyrou, G. Berginc, O. Maury, J. W. Perry, C. Andraud, *Phys. Chem. Chem. Phys.* **2012**, *14*, 15299–15307.

Received: February 20, 2013

Revised: March 27, 2013

Published online: ■■■, 0000